

ADSORPTION OF MOLECULAR HYDROGEN ON NANOSTRUCTURED SURFACES

ADSORCIÓN DE HIDRÓGENO MOLECULAR SOBRE SUPERFICIES NANOESTRUCTURADAS

A. MARTÍNEZ-MESA^{a†} AND G. SEIFERT^{b‡}

a) Facultad de Física, Universidad de La Habana, Cuba. aliezer@sica.uh.cu[†]

b) Institut für Physikalische Chemie, Technische Universität Dresden, Deutschland. gotthard.seifert@chemie.tu-dresden.de[‡]

[†] corresponding author.

(Recibido 15/03/2014; Aceptado 20/05/2014)

PACS: Quantum statistical mechanics of quantum fluids, 67.10.Fj; Hydrogen storage, 88.30.R-; Physisorption, 68.43.-h.

In recent years, many experimental and theoretical investigations have been devoted to understanding the process of light molecule adsorption in nanoporous materials [1-5]. The interest in the evaluation of molecular diffusion rates and storage capacities has been enhanced by several related technological applications like molecular sieving [6,7], reduction of carbon dioxide emissions by vehicles [8], or fuel cells [4]. In spite of being a renewable and environmentally friendly energy source, mobile applications using molecular hydrogen as fuel are presently limited by the lack of efficient lightweight hydrogen storage devices. The most widely accepted strategy to solve this problem is to adsorb hydrogen on solid materials, which requires a detailed knowledge of the fundamentals of adsorption of H₂ molecules. The investigation of the physisorption of light molecules in porous materials is also a topic of current interest from the standpoint of fundamental science. Specifically, many studies have explored the possible manifestation of macroscopic quantum effects, triggered by the confinement imposed on the adsorbates by the host structure. H₂ is the lightest molecule found in nature and it is therefore very appealing as a mean to gain deeper insight into the quantum behaviour of adsorbed molecules.

Contrary to chemisorption, in the process of physisorption the guest molecules interact only weakly with the surface of the host material by means of London dispersion forces. Hence, hydrogen molecules retain their identity upon adsorption. Due to the reversibility and fast kinetics of the physisorption process, it offers a promising alternative for developing novel hydrogen storage technologies for transport applications. The complexity of realistic porous materials, as well as other factors such as the dependence on the pretreatment of the samples, increase the difficulties associated with the interpretation of experimental data. Therefore, the theoretical modelling of the physical adsorption of molecular hydrogen plays an important role in the identification of the microscopic mechanisms governing these phenomena. Quantum effects should be explicitly incorporated in such theoretical models, since deviations from

the predictions based on classical methodologies may become noticeable even at room temperature [9, 10].

Because of the overwhelming effort required to carry out rigorous numerical simulations of the many-body quantum dynamics of adsorbates in the high-density regime, which exceeds the computational resources available nowadays, they remain as a challenging task for both theoretical and computational physics. Compared to the computationally very demanding path-integral calculations, liquid density functional theory in general and the extension to quantum fluids termed as Quantum Liquid Density Functional Theory (QLDFT) [11-13] particularly, constitutes a promising, efficient alternative technique to calculate thermophysical properties of quantum systems in condensed phases.

Concerning the rotational motion of H₂ embedded in nanostructured solids, the molecules are generally expected to behave as free rotors. In fact, the rotational barriers can influence the amount of molecular hydrogen taken in by the substrate only for materials with fairly narrow pores (e.g., rotational hindering can prevent H₂ adsorption [14, 15]). Since intramolecular vibrations can also be regarded as frozen and the electronic ground state of H₂ is characterized by a nearly spherical electron distribution, the thermophysical properties of the adsorbed fluid presented in the remainder of the paper has been computed by treating hydrogen molecules as point particles.

The aim of this work is to attain a deeper understanding of physisorption of molecular hydrogen at surfaces, explicitly accounting for quantum effects triggered by the confinement imposed by the host structure. Owing to the many-body character of the adsorption phenomena, these processes will be described by means of the QLDFT [12] and explicitly accounting for the exchange symmetry of the H₂ molecules [10,13]. The adsorption properties of the target nanostructures (carbon nanotubes (CNT), carbon foams and C₂₈ fullerites) are evaluated in a broad range of thermodynamic

conditions. The influence of both the interaction with the nanoporous environment and the quantum statistics on the adsorption isotherms is investigated. Likewise, we also focus on the microscopic spatial distribution of the adsorbed fluids and its relationship with the structural characteristics of adsorbing media. The evaluation of the thermodynamic properties of the system is carried out in the grand canonical ensemble, at constant volume V , temperature T and chemical potential μ .

Because of the featureless particle modelling of H_2 molecules, all the information about the influence of the molecular size on the adsorption process is masked into the H_2 -surface, $v_{ext}(\vec{r})$, and the H_2 - H_2 , $w(r)$, interaction potentials. The effective Hamiltonian \hat{H}_s governing the dynamics of the Kohn-Sham reference system reads

$$\hat{H}_s = -\frac{\hbar^2}{2M_{H_2}} \nabla^2 + v_{ext}(\vec{r}) + \int w(|\vec{r} - \vec{r}'|) \rho(\vec{r}') d^3\vec{r}' + v_{xc}[\rho], \quad (1)$$

where M_{H_2} and $\rho(\vec{r})$ are, respectively, the mass and the density of hydrogen molecules. The exchange-correlation potential v_{xc} is evaluated, within the Local Density Approximation, from the empirical equation of state of the homogeneous system as described in Ref. [12].

The distribution of H_2 molecules is obtained via a series expansion of the Bose-Einstein distribution function [10] in powers of the scaled and shifted effective Hamiltonian

$$\hat{\rho}_s = \frac{1}{e^{\beta(\hat{H}_s - \mu)} - 1} = \sum_{k=1}^{\infty} \sum_{m=0}^{\infty} \frac{[-k\beta(\hat{H}_s - \mu)]^m}{m!}, \quad (2)$$

where $\beta = 1/k_B T$ is the inverse temperature. The molecular density $\rho(\vec{r})$ is given by the diagonal elements of the number operator $\hat{\rho}_s$, evaluated using a three-dimensional finite-difference representation of the effective Hamiltonian \hat{H}_s . The grand potential of the interacting system is calculated using a similar procedure [10].

In the present work, a global potential energy surface for the H_2 -surface interaction is built by fitting *ab initio* calculated interaction energies [11] using the pairwise additive functional form

$$v_{ext}(\vec{r}) = \sum_i A e^{-d|\vec{r} - \vec{r}_i|} - \frac{C}{|\vec{r} - \vec{r}_i|^6}. \quad (3)$$

On the other hand, the intermolecular H_2 - H_2 interactions were modelled as Morse functions with parameters $D = 0.291 \text{ kJ}\cdot\text{mol}^{-1}$, $r_e = 3.511 \text{ \AA}$ and $\alpha = 1.592 \text{ \AA}^{-1}$ [10].

In equation (3), the vectors \vec{r}_i indicate the positions of carbon atoms in the steady carbon structure. Hence, the spatial distribution of the carbon network chiefly influences the hydrogen storage capacity of the adsorbing media via $v_{ext}(\vec{r})$. The host structures to be analyzed in this work are representative of the wide variety of thermodynamically stable carbon allotropes. Carbon nanotubes [16] are paradigmatic examples of nanostructured materials, capable to attract

hydrogen molecules on their inner and outer surfaces. The structure of carbon foams (or honeycomb graphite) [17] is similar to that of the nanotubes, but the walls of their hexagonal pores are made of interconnected graphite-like segments. The geometry of the CNT and of the carbon foams is specified in terms of the so called Hamada indexes (m,n) . On the other hand, C_{28} constitutes one of the smaller fullerenes observed experimentally [18]. Two hypothetical crystalline formations consisting in the arrangement of C_{28} cages in a lattice have been suggested, but only the one known as hyperdiamond will be considered here.

In the calculations, the unit cell was replicated along the three spatial directions until the evaluation of the effective potential was converged. Periodic boundary conditions were imposed to the Hamiltonian \hat{H}_s and the density $\rho(\vec{r})$. The molecular density is computed self-consistently using damped two-point iterations starting from the classical distribution at the specified thermodynamic conditions.

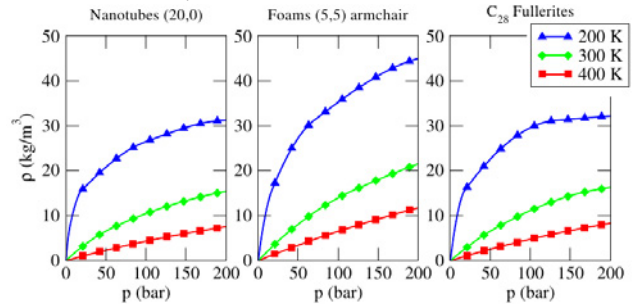


Figure 1: Average density ρ of physisorbed molecular hydrogen inside the interstitial space of selected carbon allotropes, as a function of the pressure of the external gas and at temperatures of 200 K, 300 K and 400 K.

Figure 1 illustrates the behaviour of the adsorption isotherms $\rho(p,T)$ derived within QLDFT. The average concentration of the adsorbed fluid increases as the external gas pressure gets larger, reaching a value of about $30 \text{ kg}\cdot\text{m}^{-3}$ for the selected carbon nanotubes and the fullerites, and $45 \text{ kg}\cdot\text{m}^{-3}$ for the armchair foams, at a temperature of 200 K. A fast deterioration of adsorption capacities with the increase of temperature is also striking. It is worth to notice, that the strength of the H_2 -substrate interaction potential is rather similar for the three structures ($\sim 10 \text{ kJ}\cdot\text{mol}^{-1}$). The differences in the hydrogen uptake by CNT and the (5,5) armchair foams is due to the broader spatial extension of the main adsorption sites of the latter. In the case of the C_{28} solid, despite their large attractive area, the adsorption is markedly affected by entropic contributions to the interaction free energy. Indeed, the free energy of a bound H_2 molecule at room temperature is approximately $5 \text{ kJ}\cdot\text{mol}^{-1}$, whereas this magnitude approaches $8 \text{ kJ}\cdot\text{mol}^{-1}$ for the other materials addressed here. The deviations in the H_2 -surface binding energy compensates the different accessible volumes for adsorption on the (20,0) nanotubes and the hyperdiamond, yielding nearly identical adsorbed hydrogen densities for both materials.

The most important quantity characterizing the ability of nanostructured surfaces to take up hydrogen is the gravimetric capacity, i.e., the ratio between the weights of adsorbed

molecules and that of the whole system (including the host structure). In figure 2, it can be seen that this quantity closely follows the general trend of the adsorption isotherms presented above. The gravimetric ratio g_w predicted for the (5,5) armchair foams (almost 6%), at a temperature of 200 K and at an external gas pressure of around 200 bar, is among the larger storage capacities found for pure carbonaceous materials. However, it shifts down to 2.5% at room temperature and at moderately large pressures. Nanotubes and fullerenes exhibit gravimetric capacities below 2% at room temperature.

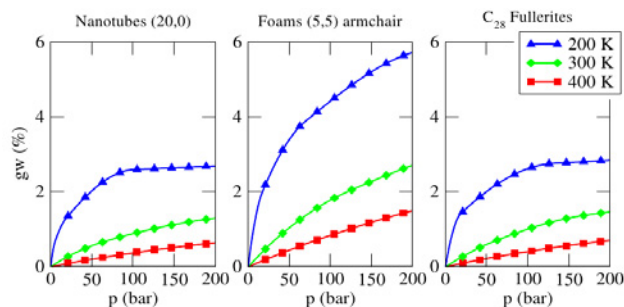


Figure 2: Gravimetric storage capacities g_w of several adsorptive media: carbon nanotubes (left panel), foams (middle panel) and C_{28} fullerenes (right panel). The storage capacity is plotted as a function of the pressure of the external gas and at temperatures of 200 K, 300 K and 400 K.

The microscopic density profiles depicted in figure 3 show the effects of augmenting the average density on the spatial distribution of the adsorbed fluid. These results correspond to the unit cell of a (4,4) armchair carbon foam at a temperature of 200 K. It can be seen, that the molecular density becomes less structured as the average concentration increases. This shows that short-range repulsive forces dominate over the attractive tail of the intermolecular potential, for these thermodynamic conditions. The enhancement of the intensity of the H_2 - H_2 repulsion causes the depletion of the heights of the peaks at the main adsorption sites (close to the corners of the pores) and the subsequent rise of the presence of H_2 molecules at the centre of the cavity.

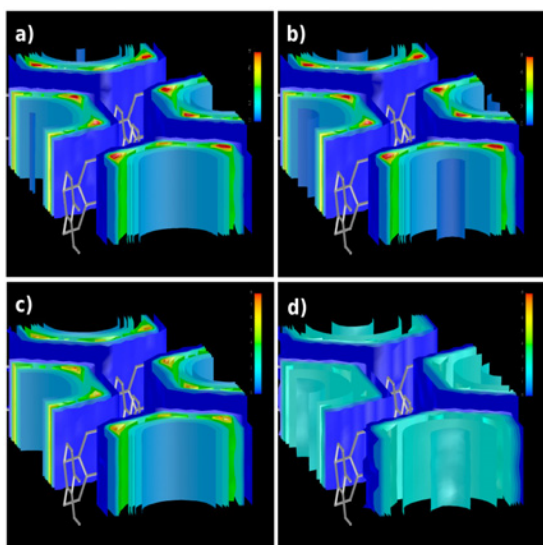


Figure 3: Contour plots of the molecular density inside the unit cell of (4,4) armchair carbon foams, at atmospheric pressure and at a temperature of 200 K. The different panels correspond to progressively larger hydrogen densities: a) $\rho = 0.0625 \text{ kg}\cdot\text{m}^{-3}$, b) $\rho = 0.625 \text{ kg}\cdot\text{m}^{-3}$, c) $\rho = 6.25 \text{ kg}\cdot\text{m}^{-3}$, and d) $\rho = 62.5 \text{ kg}\cdot\text{m}^{-3}$.

In summary, we have investigated the effect of the structural characteristics of idealized nanoporous environments on the adsorption of molecular hydrogen. The study is carried out within the density functional theory for quantum fluids at finite temperature, which allows to account for the many-body and quantum delocalization effects in a single theoretical framework, thereby enabling rigorous computer simulations of the adsorption isotherms of molecular hydrogen, and the theoretical investigation of several related phenomena in the physisorbed regime, as for example isotope separation via quantum sieving. The geometrical constraints induced by the host surface and by the intermolecular interactions, gives rise to the saturation of adsorption isotherms at large pressures and the flattening of the molecular distribution inside the material pores.

This work was supported by the DFG within the priority program "SPP 1362: Porous Metal-Organic Frameworks".

- [1] A. C. Dillon, K. M. Jones, T. A. Bekkedahl, C. H. Kiang, D. S. Bethune and M. J. Heben, *Nature* **386**, 377 (1997)
- [2] W.-Q. Deng, X. Xu, W. A. Goddard, *Phys. Rev. Lett.* **92**, 166103 (2004)
- [3] J. L. C. Rowsell and O. M. Yaghi, *J. Am. Chem. Soc.* **128**, 1304 (2006)
- [4] W.-C. Xu, K. Takahashi, Y. Matsuo, Y. Hattori, M. Kumagai, S. Ishiyama, K. Kaneko and S. Iijima, *Int. J. Hydrogen Energy* **32**, 2504 (2007)
- [5] Y. Yürüm, A. Taralp and T. Veziroglu, *Int. J. Hydrogen Energy* **34**, 3784 (2009)
- [6] Q. Wang, S. R. Challa, D. S. Sholl and J. K. Johnson, *Phys. Rev. Lett.* **82**, 956 (1999)
- [7] X. B. Zhao, S. Villar-Rodil, A. J. Fletcher and K. M. Thomas, *J. Phys. Chem. B* **110**, 9947 (2006)
- [8] L. A. Avalos, V. Bustos, R. Uac, F. Zaera and G. Zgrablich, *J. Phys. Chem. B* **110**, 24964 (2006)
- [9] J. J. M. Beenakker, V. D. Borman and S. Y. Krylov, *Chem. Phys. Lett.* **232**, 379 (1995)
- [10] A. Martínez-Mesa, S. N. Yurchenko, S. Patchkovskii, T. Heine and G. Seifert, *J. Chem. Phys.* **135**, 214701 (2011)
- [11] S. Patchkovskii and T. Heine, *Phys. Chem. Chem. Phys.* **9**, 2697 (2007)
- [12] S. Patchkovskii and T. Heine, *Phys. Rev. E* **80**, 031603 (2009)
- [13] A. Martínez-Mesa, L. Zhechkov, S. N. Yurchenko, T. Heine, G. Seifert and J. Rubayo-Soneira, *J. Phys. Chem. C* **116**, 19543 (2012)
- [14] T. Lu, E. M. Goldfield and S. K. Gray, *J. Phys. Chem. B* **110**, 1742 (2006)
- [15] G. Garberoglio, M. M. DeKlavon and J. K. Johnson, *J. Phys. Chem. B* **110**, 1733 (2006)
- [16] C. Liu and H. M. Cheng, *J. Phys. D - Applied Physics* **38**, R231 (2005)
- [17] A. Kuc and G. Seifert, *Phys. Rev. B* **74**, 214104 (2006)
- [18] X. Lu and Z. F. Chen, *Chem. Rev.* **105**, 3643 (2005)